IOP Conference Series: Materials Science and Engineering

Residual stress measurements on a deep rolled aluminum specimen through X-Ray Diffraction and Hole-Drilling, validated on a calibration bench

IOP Conf. Series: Materials Science and Engineering 1275 (2023) 012036 doi:10.1088/1757-899X/1275/1/012036

Residual stress measurements on a deep rolled aluminum specimen through X-Ray Diffraction and Hole-Drilling, validated on a calibration bench

M Beghini[1], T Grossi[1], C Santus[1], L Seralessandri[2] and S Gulisano[3]

[1] Dipartimento di Ingegneria Civile e Industriale, Università di Pisa, Pisa, Italy
[2] GNR Srl, Agrate Conturbia (NO), Italy
[3] SINT Technology Srl, Calenzano (FI), Italy

E-mail: tommaso.grossi@phd.unipi.it

Abstract. Residual stress measurements are notably affected by a high sensitivity to errors in input data. Measurements should then be presented together with an estimation of their accuracy. A common strategy is to carry out more measurements and/or to compare the results of different techniques. However, error contributions due to biases could be dangerously left unseen. In a previous work, the authors presented a calibration bench which can impose a known bending stress distribution on a specimen while simultaneously performing X-Ray Diffraction (XRD) or Hole-Drilling Method (HDM) residual stress measurements. Since the external load can freely be applied and removed, the superposition principle can be exploited to simultaneously identify either the reference bending stress distribution or the actual residual stress distribution, with the same experimental setup. A deep rolling treatment was measured and analyzed on the calibration bench with both XRD and HDM. First, residual stresses on the surface were evaluated with XRD measurements, then electrochemical material removal was performed to investigate stresses at higher depths. After that, HDM measurements were carried out and compared with the results of XRD. Both methods were also used to identify the known bending stresses, providing an additional validation of the residual stress results.

1. Introduction

Measuring residual stresses is a particularly challenging task [1]. A well-trained operator is often critical; the solution process is often grounded on a great deal of FEM calculations [2, 3, 4, 5, 6, 7] and requires the solution of an inverse problem [8, 9, 10], which is often practically ill-conditioned. The hole drilling method (HDM) [11, 12, 13, 14] is a well-known technique for measuring residual stresses, due to its low cost and its in-field applicability. It is standardized by ASTM E837 procedure [15], which can be carried out with commercially available devices, such as the MTS3000-Restan by SINT Technology. The HDM is known to be affected by a high sensitivity to noise in input data, particularly near the surface, due to the mathematical nature of the solution process. In fact, in that zone stresses depend only on the first few measurement points and are affected by errors in the identification of the zero-depth point, under the strain rosette. In addition, the ill-conditioning of the problem worsens at high depths too, where the method loses sensitivity. Due to these reasons, it is often complemented with X-Ray Diffraction (XRD) (as in [10]), which exploits Bragg's law to identify residual stresses near the specimen surface [16], with a typical penetration depth in the order of 10 µm. Stresses at higher depths

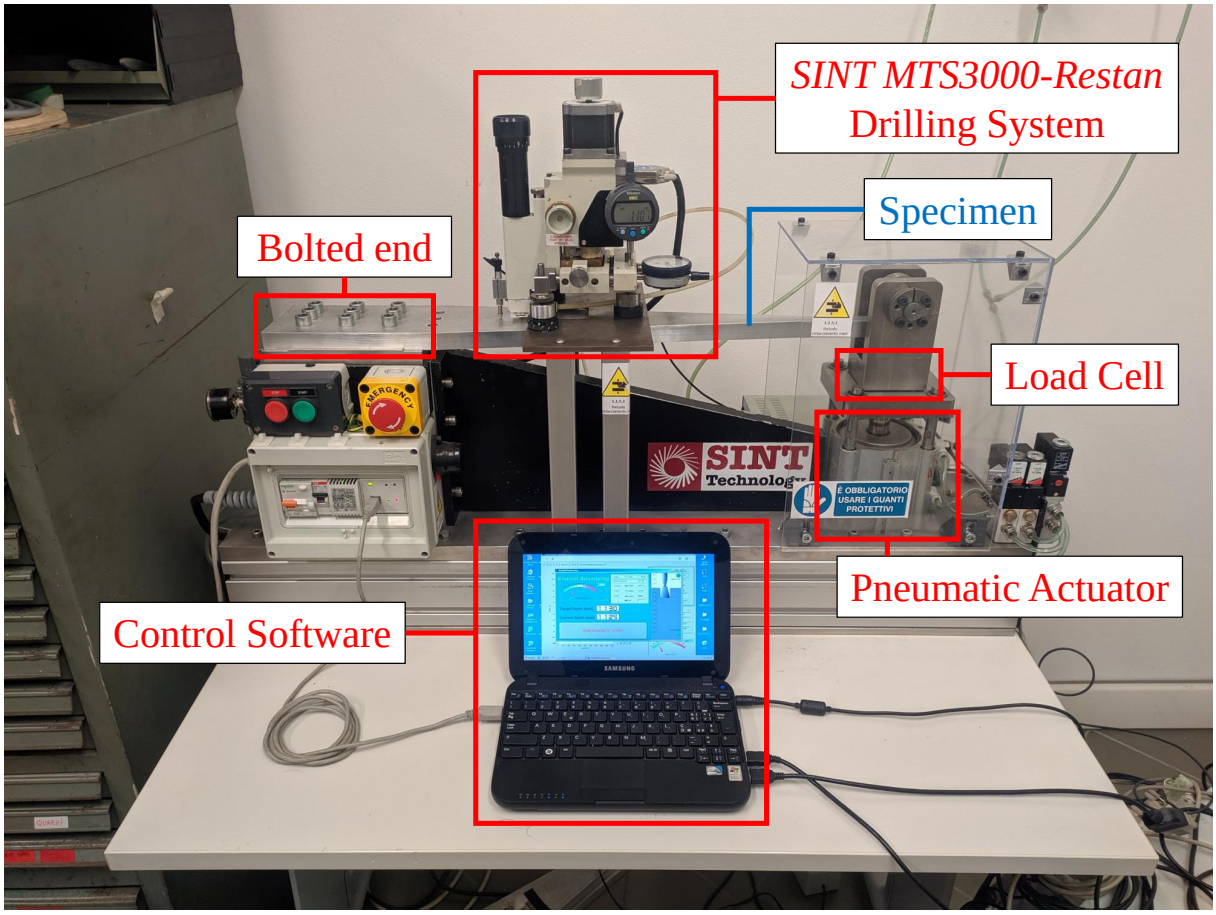

Figure 1. Description of the calibration bench.

can be profiled by removing layers of material. To this aim, electropolishing is commonly used, due to the fact that it does not introduce residual stresses in the removal process. XRD is particularly sensitive to the crystallographic properties of the material under investigation and to the strategies used to identify the diffraction peak. Therefore, its application requires a careful evaluation of the specimen and of the measurement setup, in order to gain confidence on the obtained measurements.

In a previous work [17], the authors presented a calibration bench which can impose a known bending stress distribution on a specimen while simultaneously performing X-Ray Diffraction (XRD) or Hole-Drilling Method (HDM) residual stress measurements. Most problems concerning setup, instrument calibration or material crystallographic properties generate significant differences between the reference bending distribution and its identified counterpart. Since the identification of the applied bending distribution is carried out with the same setup used to measure residual stresses, the achieved accuracy in the identification of the applied bending stresses is a direct validation of the obtained results in terms of residual stresses. For example, errors due to hole eccentricity, geometrical irregularities, zero-depth misidentification, or incorrect gauge factors are shared across the two distributions. The bench is shown in Figure 1. Details of the system are available in [17], while the decoupling procedure is described in [18]. The identification of the bending stress distribution is based on two measurements, respectively in the unloaded and in the loaded configuration. Assuming linear elasticity, the difference between the two corresponds to the effect of the applied bending

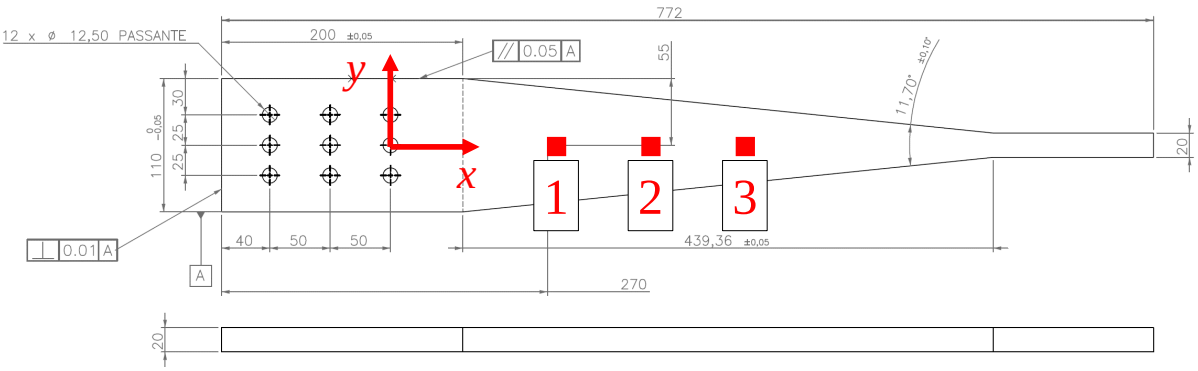

Figure 2. Technical drawing of the aluminum specimen, and definition of a reference system on its upper surface. The three measurement points are reported with red squares.

distribution alone, while measurements in the unloaded configuration corresponds to the residual stresses in the specimen.

In this work, the bench was used to analyze a deep rolling treatment on a 7075-aluminum specimen, whose technical drawing is attached in Figure 2. The corresponding residual stress distributions were analyzed through XRD and HDM measurements; both techniques were also validated on the calibration bench.

2. Methods

A deep rolling treatment was carried out on an area of $200 \times 50\,\mathrm{mm}^2$, placed along the tapered section of the specimen (see Figure 3). A tungsten carbide roller tool (model D90-L-25-0 by DREX-TOOLS) was used. The tool was mounted on a CNC machine, and its motion was numerically controlled. The normal force was measured through a load cell placed between the tool and its support, and it was manually kept at an approximately constant value of 150 N by the CNC operator, by tuning the tool position along the direction normal to the specimen surface. The same setup is described in detail in [19]. The rolling parameters are available in Table 1.

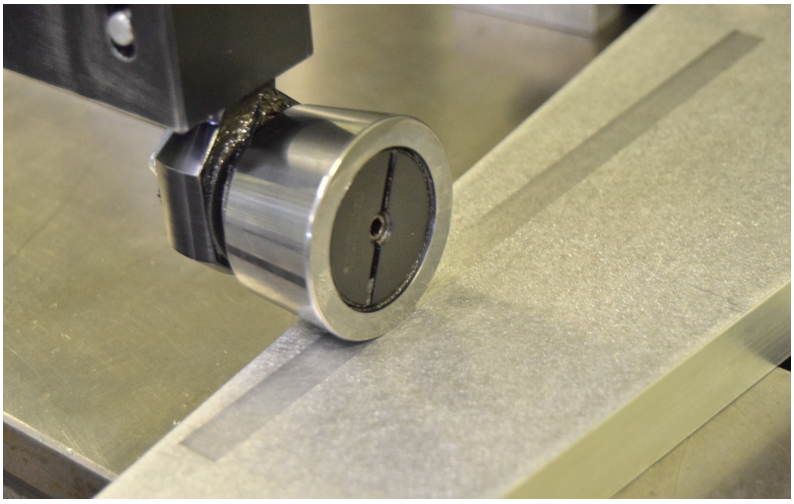

Figure 3. Photo taken during the deep rolling process, on a CNC machine.

Table 1. Tool features and deep rolling parameters

Clearance angle	Fillet radius	Feed	Normal Force
1.6°	0.78 mm	0.18 mm	150 N

A reference system on the upper surface of the specimen is defined in Figure 2. Once the specimen was mounted on the calibration bench, the corresponding bending stress distribution applied by the pneumatic actuator was accurately characterized, as described in [17]. The vertical deflections under the external load were recorded in the tapered region with an LVDT sensor, as shown in Figure 4. Through classical beam theory, this process allowed the identification of bending strains in the specimen, which were compared with values recorded by the applied strain rosette and with a FEM model. Eventually, the achieved errors on the reference distribution are reasonably at least on order of magnitude lower than typical errors in residual stress measurements, so it can practically be considered as a benchmark.

Three measurement points were placed along the specimen x axis in the tapered region (see Figure 2), then the following tests were performed:

- Near-surface XRD residual stress measurements were carried out on all three points, with a GNR SpiderX Edge diffractometer, shown in Figure 5(a). The experimental setup was validated on the calibration bench by measuring near-surface stress values of the bending

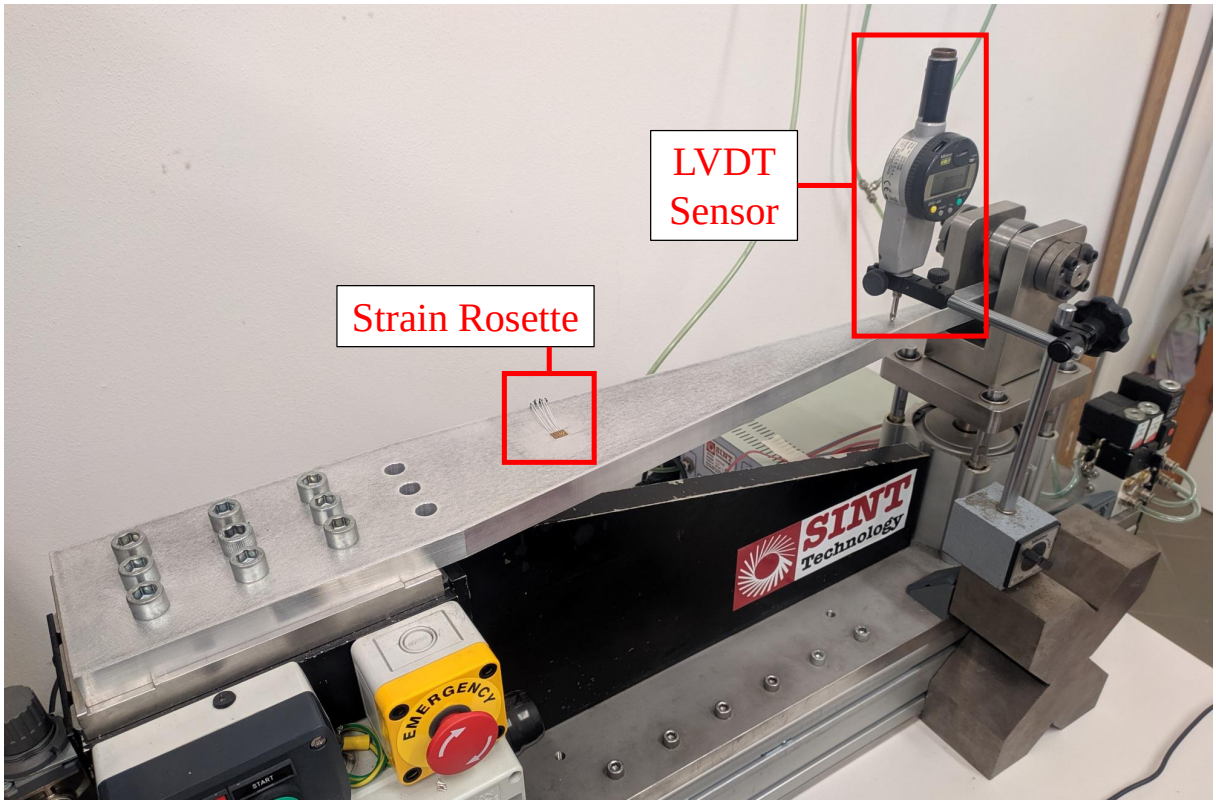

Figure 4. Specimen mounted on the calibration bench, with strain rosette applied. The vertical deflections of the specimen were measured along the whole tapered section.

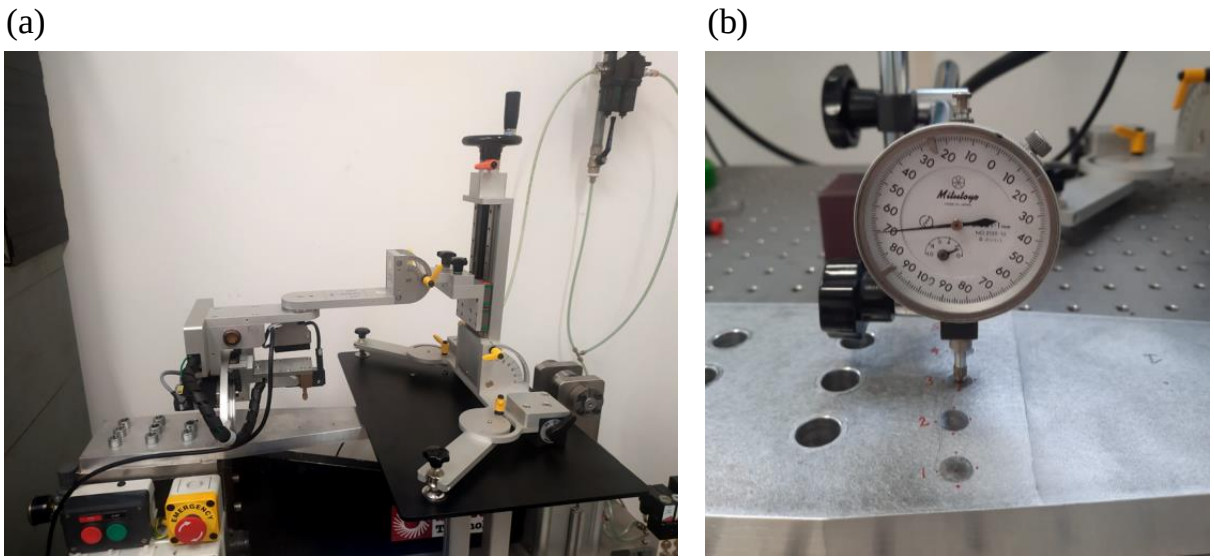

Figure 5. (a) GNR SpiderX Edge diffractometer, mounted on the calibration bench and ready to carry out a residual stress measurement. (b) Measurement of etching depth with a dial gauge.

distribution, with and without the applied load.

- HDM measurements were performed with a MTS3000-Restan system on points 1 and 2. For each drilling step, strains were sampled in both the unloaded and the loaded state, to simultaneously identify both the bending and the residual stress distribution, as mentioned before and described in [17, 18].
- XRD depth profiling through electropolishing was carried out on point 3. Diffraction measurements were performed with the same GNR SpiderX Edge diffractometer. A solution of perchloric acid was used as chemical agent. The depth was increased until clear diffraction peaks could no longer be identified.

Diffraction measurements were carried out with the $\sin 2\psi$ method, using a chrome anode

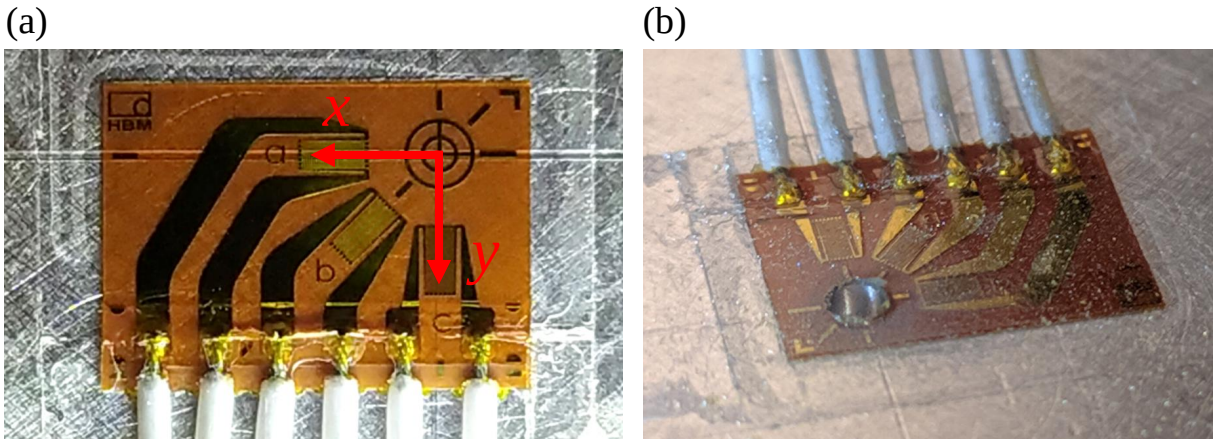

Figure 6. (a) Alignment of the strain rosette (HBM RY61K) with the specimen reference system. (b) Strain rosette applied on the upper face of the specimen, after the Hole-Drilling procedure.

and analyzing the lattice spacing of {311} planes. In order to obtain the full stress tensor without any simplifying assumption, each XRD measurement was actually performed in three directions at angles of 0°, 45° and 90° with respect to the x axis. The etching depth obtained with electropolishing was measured with a micrometer dial gauge, as shown in Figure 5(b). HBM RY61K strain rosettes were used in HDM measurements and are shown in Figure 6. Holes were drilled with an inverted cone tool having a diameter of 1.8 mm, powered by an air turbine rotating at more than 300.000 rpm. A maximum depth of 1.2 mm was reached in 120 steps of 0.01 mm. The hole diameter and eccentricity were measured through an optical microscope with crosshairs, included in the MTS3000-Restan system. Eventually, the stress distributions from 0 to 1 mm depth were obtained with the *Influence Functions* method [3, 4, 5], Tikhonov regularization and the Morozov discrepancy principle [20, 21].

3. Results

In Figure 7, the validation data for XRD near-surface measurements are reported, when only the applied bending stress distribution was identified. Each graph refers to a component of the (plane) stress tensor, extracted from the three measurements at orientations of 0°, 45° and 90°. In Figure 8, the bending stress distributions evaluated through the two HDM measurements are shown. In Figure 9, the residual stress distributions obtained with HDM measurements on points $1-2$ are compared with results from the XRD stress profiling performed on point 3.

4. Discussion

The validation process confirmed that the instrumentation setup had been properly done. In particular, XRD near-surface measurements captured the stress fields produced by the bending load with a maximum error of about 20 MPa (see Figure 7). Equivalently, HDM measurements were able to capture the bending stress distribution along the entire hole depth (see Figure 8). The achieved maximum absolute error across the whole depth range is about ±30 MPa for the largest stress component σ_{xx}, which is aligned with the state of the art [22]. Note that the error is not particularly pronounced at the surface, where HDM is instead known to be prone to higher uncertainties.

The two residual stress profiles obtained with HDM (shown in Figure 9) are consistent with the ±30 MPa maximum error achieved in the identification of the bending distribution, though at lower depths they are even more repeatable. The XRD stress profiles obtained with

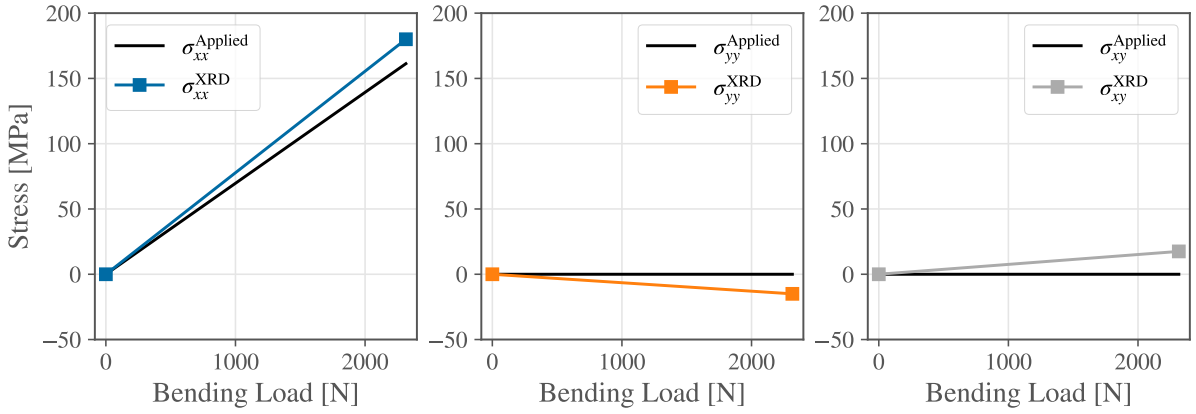

Figure 7. Validation of the XRD setup, through measurement of the reference stress fields produced by bending.

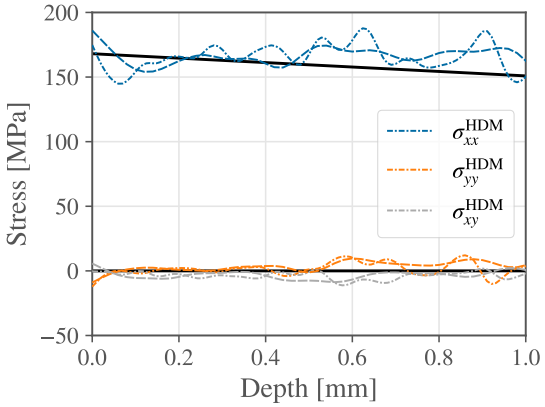

Figure 8. Bending stress fields identified through the two HDM measurements. The reference distributions are reported as black lines.

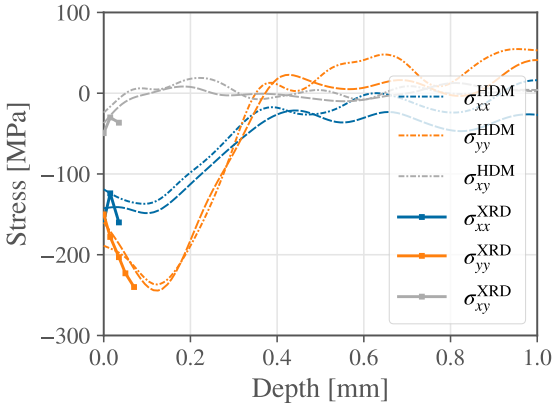

Figure 9. Obtained residual stress distributions. The HDM measurements on points $1-2$ are reported as dashed lines, while the XRD measurements on point 3 are reported as squares connected by solid lines.

electropolishing correctly mimic the trend of HDM curves, especially for the largest stresses σ_{yy}, which act in the transversal direction with respect to the rolling motion of the tool. However, the quality of the diffraction peaks quickly degraded along the depth, so the measurements turned out to be not significant after just a few removal steps. Uncertainties in the etching surface planarity probably played a role in this effect.

In addition, errors in the measurement of etching depth also affected the achieved accuracy, which was still reasonable for engineering applications. More studies will be carried out on the grain size in the specimen material and on potential texturing caused by the deep rolling process itself.

5. Conclusion

The present calibration bench allows one to validate the chosen setup before and during residual stress measurements, both with X-Ray Diffraction and the Hole-Drilling Method. For example, insufficient grain statistics, or issues in the strain gauge bonding would immediately result in huge errors in the identification of the bending distribution. Since the specimen can be designed with different materials and geometries, the calibration bench is particularly useful to investigate residual stresses produced by new surface treatments, with an increased measurement confidence provided by the validation phase.

In this work, a deep rolling treatment on a 7075-aluminum specimen was analyzed, with XRD and HDM. Both setups were validated on the calibration bench, and that allowed an estimation of the achieved accuracy on the residual stress measurements. The observed errors on the applied bending distribution are satisfactory, although the XRD depth profiling showed a rapid decrease in the quality of diffraction peaks with depth. More investigations will be carried out on the micro-structure of the specimen material.

References

[1] Schajer G S, Prime M B and Withers P J 2022 *Experimental Mechanics* ISSN 0014-4851, 1741-2765
[2] Schajer G S 1981 *Journal of Engineering Materials and Technology* **103** 157–163 ISSN 0094-4289, 1528-8889
[3] Beghini M and Bertini L 2000 *The Journal of Strain Analysis for Engineering Design* **35** 125–135 ISSN 0309-3247, 2041-3130
[4] Beghini M, Bertini L and Mori L F 2010 *Strain* **46** 324–336 ISSN 00392103, 14751305
[5] Beghini M, Bertini L and Mori L F 2010 *Strain* **46** 337–346 ISSN 00392103, 14751305
[6] Schajer G S 2020 *Experimental Mechanics* **60** 665–678 ISSN 0014-4851, 1741-2765
[7] Schajer G S 2022 *Experimental Mechanics* ISSN 0014-4851, 1741-2765
[8] Schajer G S and Prime M B 2006 *Journal of Engineering Materials and Technology* **128** 375 ISSN 00944289
[9] Smit T and Reid R 2020 *Experimental Mechanics* **60** 1301–1314 ISSN 0014-4851, 1741-2765
[10] Smit T C and Reid R G 2021 *Experimental Mechanics* **61** 1029–1043 ISSN 0014-4851, 1741-2765
[11] Lake B R, Appl F J and Bert C W 1970 *Experimental Mechanics* **10** 233–239 ISSN 0014-4851, 1741-2765
[12] Beaney E M 1976 *Strain* **12** ISSN 1475-1305
[13] Schajer G S 1988 *Journal of Engineering Materials and Technology* **110** 344–349 ISSN 0094-4289, 1528-8889
[14] Schajer G S 1992 *Strain* **28** 19–22 ISSN 00392103, 14751305
[15] American Society for Testing and Materials 2020 *West Conshohocken, PA* 10.1520/E0837-20
[16] Noyan I C and Cohen J B 2013 *Residual stress: measurement by diffraction and interpretation* (Springer) ISBN 1-4613-9570-4
[17] Beghini M, Grossi T, Santus C and Valentini E 2022 *ICRS 11–11th International Conference on Residual Stresses*
[18] Valentini E, Beghini M, Bertini L, Santus C and Benedetti M 2011 *Strain* **47** e605–e618 ISSN 00392103
[19] Beghini M, Bertini L, Monelli B, Santus C and Bandini M 2014 *Surface and Coatings Technology* **254** 175–186 ISSN 02578972
[20] Morozov V A 1984 *Methods for Solving Incorrectly Posed Problems* (New York, NY: Springer New York) ISBN 978-0-387-96059-3 978-1-4612-5280-1
[21] Schajer G S 2007 *Journal of Engineering Materials and Technology* **129** 440–445 ISSN 0094-4289, 1528-8889
[22] Schajer G S 2013 *Practical residual stress measurement methods* (John Wiley & Sons) ISBN 1-118-34237-2